Arch. Mech., **65**, 6, pp. 485–509, Warszawa 2013

Axi-symmetric motion of a porous approximate sphere in an approximate spherical container

D. SRINIVASACHARYA[1)], M. KRISHNA PRASAD

Department of Mathematics
National Institute of Technology
Warangal-506 004, A.P., India
[1)] *e-mail: dsc@nitw.ac.in, dsrinivasacharya@yahoo.com*

THE CREEPING MOTION of a porous approximate sphere at the instant it passes the center of an approximate spherical container with Ochoa-Tapia and Whitaker's stress jump boundary condition has been investigated analytically. The Brinkman's model for the flow inside the porous approximate sphere and the Stokes equation for the flow in an approximate spherical container were used to study the motion. The stream function (and thus the velocity) and pressure (both for the flow inside the porous approximate sphere and inside an approximate spherical container) are calculated. The drag force experienced by the porous approximate spherical particle and wall correction factor are determined in closed forms. The special cases of porous sphere in a spherical container and oblate spheroid in an oblate spheroidal container are obtained from the present analysis. It is observed that drag not only changes with the permeability of the porous region, but as the stress jump coefficient increases, the rate of change in behavior of drag increases.

Key words: porous approximate sphere, Stokes flow, Brinkman equation, stress jump coefficient, drag, wall correction factor.

Copyright © 2013 by IPPT PAN

1. Introduction

THE PROBLEMS OF THE MOTION of a particle at the instant it passes the center of the spherical container serves as a model of interaction in multi-particle systems. This class of problems is important because it provides some information on wall effects. Wall effects for a sphere at the instant it passes the center of the spherical container have been studied by many authors and these studies were summarized by OSEEN [1], HAPPEL and BRENNER [2], KIM and KARRILA [3], and JONES [4]. A survey of literature regarding the fluid flows past and within porous bodies indicates that while abundant information is available for flows in an infinite expanse of fluid, very little information is available for flows in enclosures. CUNNINGHAM [5] and WILLIAMS [6], independently, considered the motion of a solid sphere in a spherical container. HABERMAN and SAYRE [7] have made an analogous study for the motion of an inner Newtonian fluid sphere.

Ramkissoon and Rahaman investigated the motion of inner non-Newtonian (Reiner–Revlin) fluid sphere in a spherical container [8] and a solid spherical particle in a spheroidal container [9]. The problem of Stokeslet outside a rigid spherical particle was first solved by Oseen [1]. Maul and Kim [10, 11] studied the Stokes equations for a point force in a fluid domain bounded by a rigid spherical container and the image of a point force in a spherical container and its connection to the Lorentz reflection formula. A spherical envelope approach to ciliary propulsion was studied by Blake [12]. The Stokes mobility functions for translation and rotation of the spherical particle in a spherical cavity is investigated by Felderhof and Sellier [13]. The flow problems of the motion of a porous particles in a container have been modeled by using Stokes' version of the Navier–Stokes equations for the flow inside the container and Darcy's law or Brinkman's equation to describe the flow within the porous particles.

Joseph and Tao [14] considered the creeping flow past a porous spherical shell immersed in a uniform viscous incompressible fluid using Darcy's law for the flow inside the porous region and Stokes equations for the fluid outside the sphere. They have taken the boundary conditions as continuity of normal velocity and pressure at the surface of the porous sphere and no-slip of tangential velocity component of the free fluid. They found that the drag on the porous sphere is the same as that of a rigid sphere with reduced radius. The usage of no-slip condition at the permeable surface was not satisfactory and indeed a slip occurs at the boundary as shown by Beavers and Joseph [15]. To accommodate this, they proposed a slip boundary condition for plane boundaries is

$$\frac{\partial u}{\partial y} = \frac{\lambda}{\sqrt{k}}(u - Q),$$

where u is the velocity parallel to the surface, y is the coordinate normal to the surface, Q is the velocity inside the porous medium, k is the permeability and λ is a dimensionless constant whose value depends on the properties of the porous medium. Their experimental values showed a reasonable agreement with the values predicted by this condition. Using a statistical approach to extend Darcy's law to non-homogeneous porous media, Saffman [16] gave a theoretical justification of the condition proposed by Beavers and Joseph [15]. He showed that in the limit $k \to 0$

$$u = \frac{\sqrt{k}}{\lambda}\frac{\partial u}{\partial y} + O(k)$$

at the boundary. For small values of k, Saffman's condition is more appropriate than the usual no-slip condition.

Using Saffman's boundary conditions at the surface of the sphere, Padmavathi *et al.* [17] have studied the creeping flow past a porous sphere immersed in a uniform viscous incompressible fluid using Darcy's law. It was shown

therein that the torque on a porous sphere is always less than that on a rigid sphere, whereas the drag in general is not. On the other hand, Sutherland and Tan [18] have used the continuity of normal velocity, pressure and the tangential velocity component.

However Darcy's law appears to be inadequate for the flows with high porosity, and large shear rates and for flows near the surface of the bounded porous medium. To model such flows a modification of Darcy's law was proposed by Brinkman [19] and Debye and Bueche [20] independently. The validity of this equation was confirmed by experimental verification of Ooms *et al.* [21] and Matsumoto and Suganuma [22] and theoretically justified by Tam [23] and Lundgren [24]. Qin and Kaloni [25] considered the creeping flow past and through a porous sphere using Brinkman's law for the flow inside the porous region and Stokes equations for the fluid outside the sphere. Zlatanovski [26] has studied the axisymmetric flow past a porous prolate spheroidal particle using the Brinkman model for the flow inside the spheroidal particle and Stokes model for the free flow region. The quasisteady translation and steady rotation of a spherically symmetric composite particle composed of a solid core and a surrounding porous shell located at the center of a spherical cavity filled with an incompressible Newtonian fluid is studied by Keh and Chou [27]. The quasisteady translation and steady rotation of a spherically symmetric porous shell located at the center of a spherical cavity filled with an incompressible Newtonian fluid is investigated analytically by Keh and Lu [28]. The motion of a porous sphere in a spherical container using Brinkman's model in the porous region was studied by Srinivasacharya [29]. The solution of the problem of symmetrical creeping flow of an incompressible viscous fluid past a swarm of porous approximately spheroidal particles with Kuwabara boundary condition (i.e., the vanishing of vorticity on the boundary) is investigated by Deo and Gupta [30]. The flow problem of an incompressible axisymmetrical quasisteady translation and steady rotation of a porous spheroid in a concentric spheroidal container are studied analytically by Saad [31]. All these authors [25]–[31] have used continuity of the velocity, pressure and tangential stresses at the porous-liquid interface. This continuity of both velocity and stress (built on the effective viscosity) at the interface is easily achieved since the Brinkman equation and the Stokes equation are of the same order. Nield [32] pointed out that the continuity of stress at the interface is clearly valid at the microscopic level (in the pores) but not necessarily for the average macroscopic stress. Tomar and Uri [33] showed that planar averaging of the microscopic solution exhibits a continuous shear stress within the fluid phase and within the porous phase. This continuity breaks down when moving from the fluid to the porous domain across a sharp interface, due to a momentum transfer to the solid phase which occurs below the interface but absent above it. Ochoa-Tapia and Whitaker [34, 35] reasoned

that due to spatial changes of the local porous structure that characterize the interface region, the macroscopic conservation equations in both homogeneous fluid and porous regions may not be satisfied. In order to handle this difficulty in the context of volume averaging, they have developed the momentum transfer condition at the boundary between a porous medium and a homogeneous fluid as a jump condition. This is known as stress jump boundary condition and is given by

$$\epsilon^{-1}\frac{\partial u^p}{\partial y} - \frac{\partial u^l}{\partial y} = \frac{\sigma}{\sqrt{k}}u^p,$$

where u^p, u^l are tangential velocity components in porous region and liquid region respectively, ϵ is the porosity, k is the permeability of the homogeneous portion of the porous region and σ is the stress jump coefficient. If $\sigma \neq 0$, there is a discontinuity in the shear stress at the porous-liquid interface. This jump condition is constructed to join Darcy's law with the Brinkman correction to Stokes equations. Experimentally it has been verified that the jump coefficient σ varies in the range -1 to 1 [34–37]. Kuznetsov [36, 37] used this stress jump boundary condition at the interface between a porous medium and a clear fluid to discuss flow in channels partially filled with porous medium. Valdés-Parada *et al.* [38] have computed the jump coefficient for unidirectional channel flow, where it is shown that the jump coefficient explicitly depends on porosity and Darcy number ($Da = k/a^2$). Raja Sekhar and Bhattacharyya [39] used stress jump boundary condition while discussing the Stokes flow of a viscous fluid inside a sphere with internal singularities, enclosed by a porous spherical shell. They concluded that the fluid velocity at a porous-liquid interface varies with the stress jump coefficient.

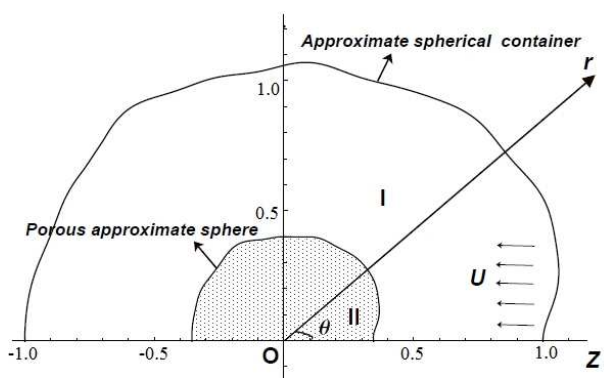

Fig. 1. The physical situation and the coordinate system ($m = 20$, $a = 1$, $b = 0.4$). The equation of the porous approximate sphere is $r = a[1 + \sum_{m=2}^{\infty} \beta_m \vartheta_m(\zeta)] \equiv r_a$. The equation of an approximate spherical container is $r = b[1 + \sum_{m=2}^{\infty} \gamma_m \vartheta_m(\zeta)] \equiv r_b$.

In this paper, we consider the creeping motion of a porous approximate sphere at the instant it passes the center of an approximate spherical container. We have used the Brinkman's model for the flow inside the porous approximate sphere and Stokes' model for the flow within the approximate spherical container. As boundary conditions, continuity of the velocity, pressure and the slip condition at the interface proposed by Ochoa-Tapia are employed. The stream function and the pressure for both the flows inside porous particle and within an approximate spherical container are calculated to the first order in the small parameter characterizing the deformation. The drag experienced by the porous approximate sphere and wall effects are studied numerically.

2. Formulation of the problem

Consider a porous approximate spherical particle passing the center of an approximate spherical vessel containing an incompressible Newtonian viscous fluid. This is equivalent to the inner particle at rest while the outer approximate spherical container moves with a constant velocity $\mathbf{U}$ in the negative Z-direction. The porous medium is assumed to be homogeneous and isotropic. Let (r, θ, ϕ) denote a spherical polar co-ordinate system with the origin at the center of the sphere of radius a.

Let the equation of the inner (porous) approximate sphere be

$$r = a\Big[1 + \sum_{m=2}^{\infty} \beta_m \vartheta_m(\zeta)\Big] \equiv r_a$$

and an approximate spherical container be

$$r = b\Big[1 + \sum_{m=2}^{\infty} \gamma_m \vartheta_m(\zeta)\Big] \equiv r_b,$$

where the β_m and γ_m are small, $\zeta = \cos\theta$, $\vartheta_m(\zeta)$ is the Gegenbauer function [2] of the first kind of order m and degree $-1/2$. If all the β_m and γ_m are zero, the approximate spheres reduce to spheres of radii a and b. The liquid region $(r_a \le r \le r_b)$ and the porous region $(r \le r_a)$ are denoted by regions I and II respectively. We assume that the flow within an approximate spherical container is the Stokesian, and Brinkman's law [19] governs the flow inside the porous approximate sphere.

The equations of motion for the region within an approximate spherical container (region I) are

$$\nabla \cdot \mathbf{q}^{(1)} = 0, \tag{2.1}$$

$$\nabla p^{(1)} + \mu \nabla \times \nabla \times \mathbf{q}^{(1)} = 0, \tag{2.2}$$

where $\mathbf{q}^{(1)}$ is the volumetric average of the velocity, μ is the coefficient of viscosity and $p^{(1)}$ is the average of the pressure.

For the region inside the porous approximate sphere (region II), the equations of motion are

$$\nabla \cdot \mathbf{q}^{(2)} = 0, \tag{2.3}$$

$$\nabla p^{(2)} + \frac{\mu}{k}\,\mathbf{q}^{(2)} + \mu \nabla \times \nabla \times \mathbf{q}^{(2)} = 0, \tag{2.4}$$

where $\mathbf{q}^{(2)}$ is the volumetric average of the velocity, μ is the coefficient of viscosity, $p^{(2)}$ is the average of the pressure, and k is the permeability of the porous medium.

Since the flow of the fluid is in the meridian plane and the flow is axially symmetric, all the physical quantities are independent of ϕ. Hence, we assume that the velocity vectors $\mathbf{q}^{(1)}$ and $\mathbf{q}^{(2)}$ in the form

$$\mathbf{q}^{(i)} = u^{(i)}(r,\theta)\,\mathbf{e}_r + v^{(i)}(r,\theta)\,\mathbf{e}_\theta, \qquad i = 1,2, \tag{2.5}$$

where $(\mathbf{e}_r, \mathbf{e}_\theta, \mathbf{e}_\phi)$ are unit base vectors in spherical polar co-ordinates.

Introducing the stream functions $\psi^{(i)}(r,\theta)$, $i = 1,2$, through

$$u^{(i)} = -\frac{1}{r^2 \sin\theta}\frac{\partial \psi^{(i)}}{\partial \theta}, \qquad v^{(i)} = \frac{1}{r \sin\theta}\frac{\partial \psi^{(i)}}{\partial r}, \qquad i = 1,2, \tag{2.6}$$

in (2.2) and (2.4) and eliminating pressure from the resulting equations, we get the following dimensionless equations for $\psi^{(i)}$, $i = 1,2$:

$$E^4\,\psi^{(1)} = 0, \tag{2.7}$$

$$E^2\,(E^2 - \alpha^2)\,\psi^{(2)} = 0, \tag{2.8}$$

where $\alpha^2 = a^2/k$ and $E^2 = \dfrac{\partial^2}{\partial r^2} + \dfrac{(1-\zeta^2)}{r^2}\dfrac{\partial^2}{\partial \zeta^2}$ is the Stokesian stream function operator.

3. Boundary conditions

To determine the flow velocity and pressure outside and inside the porous approximate sphere, we use the following boundary conditions:

(i) The normal velocity component is continuous at the boundary of the approximate sphere,

$$u^{(1)}(r,\theta) = u^{(2)}(r,\theta) \qquad \text{on } r = r_a. \tag{3.1}$$

(ii) The tangential velocity component is continuous at the boundary of the approximate sphere,

$$v^{(1)}(r,\theta) = v^{(2)}(r,\theta) \qquad \text{on } r = r_a. \tag{3.2}$$

(iii) Continuity of the pressure distributions at the boundary of the approximate sphere,

$$p^{(1)}(r,\theta) = p^{(2)}(r,\theta) \qquad \text{on } r = r_a. \tag{3.3}$$

(iv) Ochoa-Tapia's stress jump boundary condition for tangential stress,

$$\frac{\partial v^{(2)}}{\partial r} - \frac{\partial v^{(1)}}{\partial r} = \frac{\sigma}{\sqrt{k}} v^{(2)} \qquad \text{on } r = r_a, \tag{3.4}$$

where σ is the stress jump coefficient. σ is a constant of order one and the sign of σ may either be positive or negative.

On the outer sphere, the condition of impenetrability leads to

$$u^{(1)}(r,\theta) = -U\cos\theta \quad \text{and} \quad v^{(1)}(r,\theta) = U\sin\theta \qquad \text{on } r = r_b, \tag{3.5}$$

and the condition that velocity and pressure must have no singularities anywhere in the flow field.

The boundary conditions from Eqs. (3.1) to (3.5) in terms of the stream function in dimensionless form are

$$\left.\begin{aligned} &\psi^{(1)}(r,\theta) = \psi^{(2)}(r,\theta), \quad \psi_r^{(1)}(r,\theta) = \psi_r^{(2)}(r,\theta) \\ &\psi_{rr}^{(2)} - \psi_{rr}^{(1)} = \alpha\,\sigma\,\psi_r^{(2)}, \quad p^{(1)}(r,\theta) = p^{(2)}(r,\theta) \end{aligned}\right\} \quad \text{on } r = 1 + \beta_m \vartheta_m(\zeta), \tag{3.6}$$

and

$$\psi^{(1)}(r,\theta) = \frac{1}{2} r^2 \sin^2\theta, \quad \psi_r^{(1)}(r,\theta) = r\sin^2\theta \qquad \text{on } r = (1/\eta)[1 + \gamma_m \vartheta_m(\zeta)], \tag{3.7}$$

where $\eta = a/b$.

4. Solution of the problem

For the region I, the solution of (2.7) which is nonsingular everywhere in the flow region is

$$\psi^{(1)} = \sum_{n=2}^{\infty} [A_n\, r^n + B_n\, r^{-n+1} + C_n\, r^{n+2} + D_n\, r^{-n+3}]\vartheta_n(\zeta), \tag{4.1}$$

For the region II, the solution of (2.8) which is finite as $r \to 0$ is given by

$$\psi^{(2)} = \sum_{n=2}^{\infty} [E_n\, r^n + F_n \sqrt{r}\, I_{n-1/2}(\alpha r)]\vartheta_n(\zeta), \tag{4.2}$$

where $I_{n-1/2}(\alpha r)$ denotes the modified Bessel function of the first kind of order $n-1/2$. Using Eqs. (4.1) and (4.2), the expressions for the pressure in the both flow regions are

$$p^{(1)} = -\sum_{n=2}^{\infty} \left[C_n \left(\frac{4n+2}{n-1} \right) r^{n-1} - D_n \left(\frac{6-4n}{n} \right) r^{-n} \right] P_{n-1}(\zeta), \tag{4.3}$$

$$p^{(2)} = \alpha^2 \sum_{n=2}^{\infty} E_n \left(\frac{r^{n-1}}{n-1} \right) P_{n-1}(\zeta), \tag{4.4}$$

where P_n is the Legendre function of first kind.

We first propose to develop the solution corresponding to the boundaries $r = 1+\beta_m\, \vartheta_m(\zeta)$ and $r = (1/\eta)[1+\gamma_m \vartheta_m(\zeta)]$. Assume that the coefficients β_m and γ_m are sufficiently small so that squares and higher powers of β_m and γ_m can be neglected [2], i.e., $r^y \approx 1+y\beta_m\vartheta_m(\zeta)$ and $r^y \approx (1/\eta^y)[1+y\gamma_m\vartheta_m(\zeta)]$, where y is positive or negative. Comparison of Eqs. (4.1) and (4.2) with those obtained in case of flow of an incompressible viscous fluid past a porous sphere in spherical container [27, 29], indicates that the terms involving A_n, B_n, C_n, D_n, E_n and F_n for $n > 2$ are the extra terms which are not present in case of sphere. The body that we are considering now is an approximate sphere and the flow generated is not expected to be much different from the one generated by flow past a porous sphere. Also the coefficients A_n, B_n, C_n, D_n, E_n and F_n for $n > 2$ are of order β_m and the coefficients A_n, B_n, C_n and D_n for $n > 2$ are of order γ_m. Therefore, while implementing the boundary conditions, we ignore the departure from the spherical form and set in (3.6) $r = 1$ in the terms involving A_n, B_n, C_n, D_n, E_n and F_n for $n > 2$ and in (3.7) $r = 1/\eta$ in the terms involving A_n, B_n, C_n and D_n for $n > 2$.

Applying the boundary conditions (3.6) and (3.7) to the first order in β_m and γ_m, we have evaluated all the coefficients appearing in the stream functions (4.1) and (4.2). These coefficients are mentioned in the Appendix. Thus, the stream functions for the regions I and II are given by

$$\begin{aligned} \psi^{(1)} &= [A_2 r^2 + B_2 r^{-1} + C_2 r^4 + D_2 r]\vartheta_2(\zeta) \\ &+ \sum_{m=2}^{\infty} \{[A_{m-2} r^{m-2} + B_{m-2} r^{-m+3} + C_{m-2} r^m + D_{m-2} r^{-m+5}]\vartheta_{m-2}(\zeta) \\ &+ [A_m r^m + B_m r^{-m+1} + C_m r^{m+2} + D_m r^{-m+3}]\vartheta_m(\zeta) \\ &+ [A_{m+2} r^{m+2} + B_{m+2} r^{-m-1} + C_{m+2} r^{m+4} + D_{m+2} r^{-m+1}]\vartheta_{m+2}(\zeta)\}, \end{aligned} \tag{4.5}$$

$$\begin{aligned}\psi^{(2)} &= [E_2 r^2 + F_2\sqrt{r}\, I_{3/2}(\alpha r)]\vartheta_2(\zeta) \\ &+ \sum_{m=2}^{\infty}\{[E_{m-2}r^{m-2} + F_{m-2}\sqrt{r}\, I_{m-5/2}(\alpha r)]\vartheta_{m-2}(\zeta) \\ &+ [E_m r^m + F_m\sqrt{r}\, I_{m-1/2}(\alpha r)]\vartheta_m(\zeta) + [E_{m+2}r^{m+2} \\ &+ F_{m+2}\sqrt{r}\, I_{m+3/2}(\alpha r)]\vartheta_{m+2}(\zeta)\}.\end{aligned} \tag{4.6}$$

Hence velocity components are determined. In case the porous approximate sphere is $r = a[1 + \sum_{m=2}^{\infty}\beta_m\vartheta_m(\zeta)]$ and approximate spherical container is $r = b[1 + \sum_{m=2}^{\infty}\gamma_m\vartheta_m(\zeta)]$, we employ the above technique for each m and obtain the expressions for the stream functions for the regions I, and II by superimposition of the expressions thus obtained.

5. Drag on the body and wall effects

The drag experienced by the inner approximate sphere is given by

$$D = \mu\pi\int_0^{\pi}\varpi^3\frac{\partial}{\partial r}\left(\frac{E^2\psi^{(1)}}{\varpi^2}\right) r\, d\theta, \tag{5.1}$$

where $\varpi = r\sin\theta$.

Using Eq. (4.1) and carrying out the integration it is found that

$$D = 4\pi\mu U a[D_2 + D_2'], \tag{5.2}$$

where D_2 and D_2' are given in Appendix. The coefficients D_2 and D_2' are the Stokeslet coefficients of the stream function (4.1), which only contribute to the drag force.

As $b \to \infty$ (or $\eta \to 0$), we get the drag on a porous approximate sphere in the case of streaming in an unbounded medium,

$$D_\infty = 4\pi\mu U a\left[\left(\Delta_7 + \frac{1}{5}\Delta_8\beta_2 + \frac{2}{35}\Delta_9\beta_4\right)/\Delta_6\right], \tag{5.3}$$

where Δ_6, Δ_7, Δ_8, Δ_9 are given in Appendix.

It is interesting to note that although the boundary surface is given by $r = a[1 + \sum_{m=2}^{\infty}\beta_m\vartheta_m(\zeta)]$ and $r = b[1 + \sum_{m=2}^{\infty}\gamma_m\vartheta_m(\zeta)]$, only the coefficients β_2, β_4, γ_2 and γ_4, contribute to the drag. This implies that the drag on the porous approximately spherical shell is relatively insensitive to the details of the surface geometry. This is similar to the observation made by SRINIVASACHARYA [40].

The changes of shape from porous sphere to porous approximate sphere and spherical container to approximate spherical container are shown in Fig. 2. The

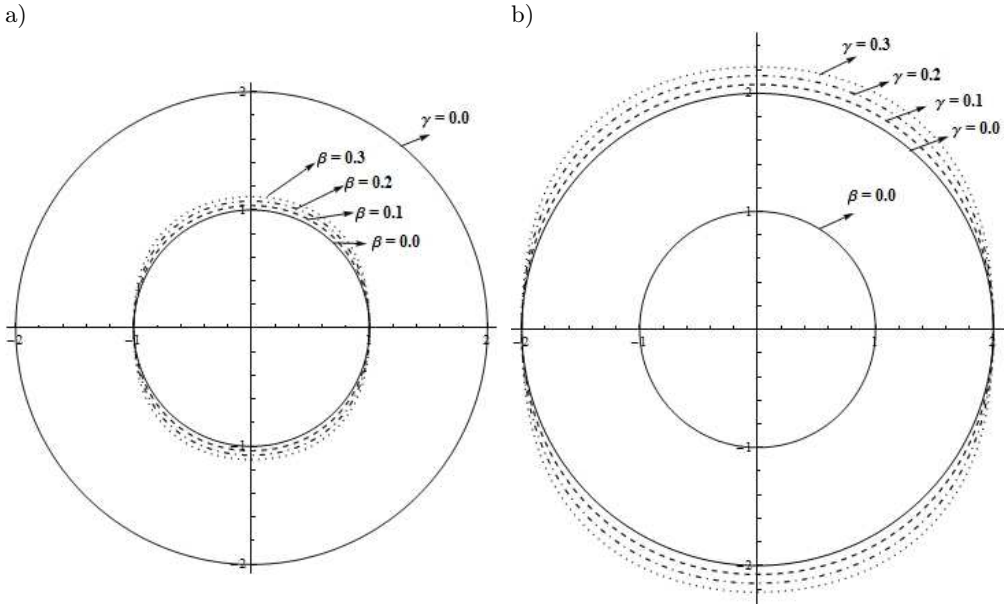

Fig. 2. The shape of the body with varying deformation parameters of the inner sphere ($\beta_2 = \beta_4 = \beta$), the outer sphere ($\gamma_2 = \gamma_4 = \gamma$) and the separation parameter $\eta = 0.5$.

variation of the drag coefficient $D_N = D/(4\pi\mu U a)$ for various values of normalized permeability k_1 $(= 1/\alpha^2)$, the inner deformation parameter β $(\beta_2 = \beta_4 = \beta)$, and the outer deformation parameter γ $(\gamma_2 = \gamma_4 = \gamma)$ with no effect of the stress jump coefficient $(\sigma = 0)$ is shown in Fig. 3. From Fig. 3a, it is observed that the drag coefficient is decreasing as the permeability is increasing. There is a slight increase in the drag coefficient as the deformation parameter of the porous sphere

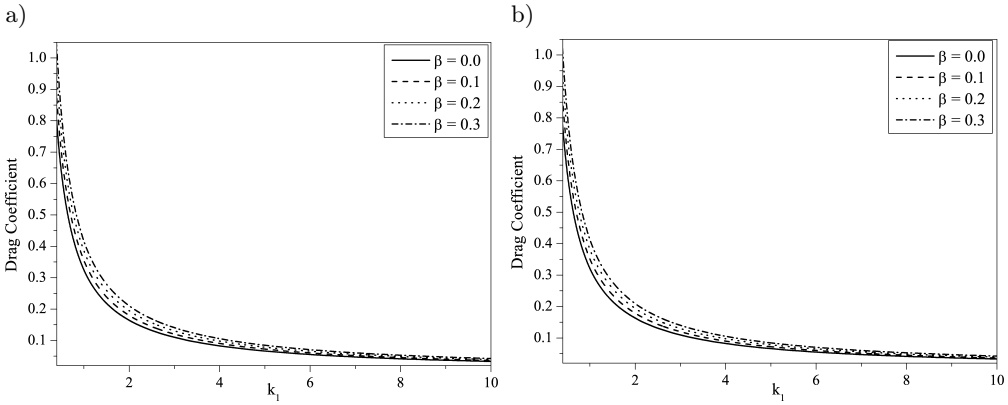

Fig. 3. Variation of the drag coefficient D_N with normalized permeability k_1 for various values of β: a) $\gamma = 0.0$, $\sigma = 0$, $\eta = 0.6$; b) $\gamma = 0.15$, $\sigma = 0$, $\eta = 0.6$.

(β) is increasing. It is interesting to note that the drag coefficient on the porous sphere is less than the one on porous approximate sphere in presence of spherical cavity. Figure 3b shows the variation of the D_N with the deformation of the porous sphere (β) when the spherical container is perturbed ($\gamma = 0.15$). It is noticed that there is a slight decrease in the drag on the porous approximate particle as the deformation of the outer sphere γ increases. This variation of the drag coefficient D_N with normalized permeability k_1 can be seen in Tables 1 and 2.

Table 1. Variation of the drag coefficient D_N with normalized permeability k_1 for various values of β; $\gamma = 0.0$, $\sigma = 0$, $\eta = 0.6$.

	Drag coefficient			
k_1	$\beta = 0.0$	$\beta = 0.1$	$\beta = 0.2$	$\beta = 0.3$
0.5	0.62879	0.69042	0.75205	0.81367
1	0.32347	0.35421	0.38494	0.41568
5	0.06626	0.07238	0.07851	0.08463
7	0.04741	0.05178	0.05616	0.06053
10	0.03323	0.03629	0.03935	0.04241

Table 2. Variation of the drag coefficient D_N with normalized permeability k_1 for various values of β; $\gamma = 0.15$, $\sigma = 0$, $\eta = 0.6$.

	Drag coefficient			
k_1	$\beta = 0.0$	$\beta = 0.1$	$\beta = 0.2$	$\beta = 0.3$
0.5	0.61557	0.67719	0.73882	0.80044
1	0.31993	0.35067	0.38140	0.41214
5	0.06611	0.07223	0.07836	0.08448
7	0.04733	0.05171	0.05608	0.06045
10	0.03319	0.03625	0.03931	0.04238

The effect of the stress jump coefficient σ and normalized permeability k_1 on drag coefficient D_N at the porous-liquid interface has been plotted in Fig. 4. It is observed that the drag is decreasing as the stress jump coefficient σ is increasing. The drag is decreasing as the permeability is increasing when there is a jump in the stress at the boundary. For positive values of stress jump coefficient σ, there is a reversal in the behavior of drag at a particular value of permeability (critical permeability [39]). Beyond the value of critical permeability, the value of drag becomes negative which is not physically possible. Therefore, the positive values of σ cannot be considered beyond that particular critical permeability.

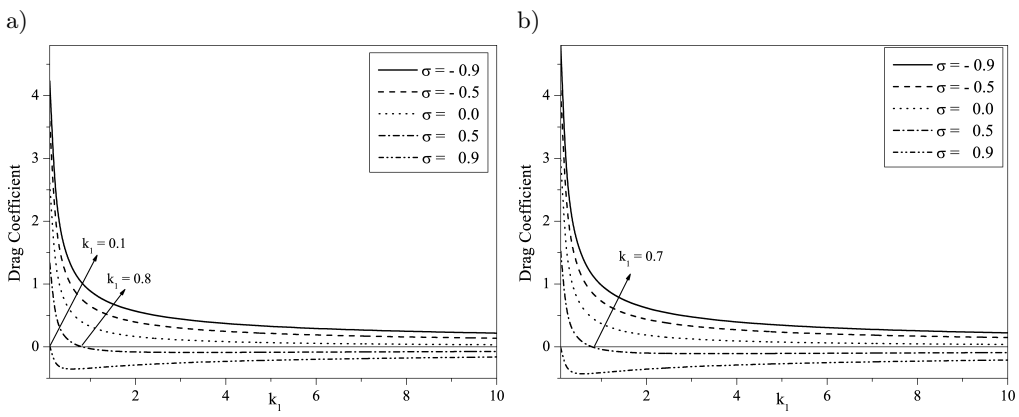

Fig. 4. Variation of the drag coefficient D_N with normalized permeability k_1 for various values of σ: a) $\beta = 0.0$, $\gamma = 0.0$, $\eta = 0.6$; b) $\beta = 0.15$, $\gamma = 0.1$, $\eta = 0.6$.

If negative σ is considered in the stress jump condition (3.4) the shear stress of external free flow region becomes more than that of the porous region which generates a significant drag force on the porous surface for any permeability. But, for positive values of σ, although the shear stress of the external region becomes low, for particular range of permeability a significant drag force generates on the surface. There is a slight increase in the drag coefficient as the deformation parameters β and γ increases.

The variation of drag coefficient D_N with normalized permeability k_1 for various values of η is shown in Fig 5. Figure 5a, shows the variation of the drag for motion of porous sphere in a spherical container with no effect of stress jump

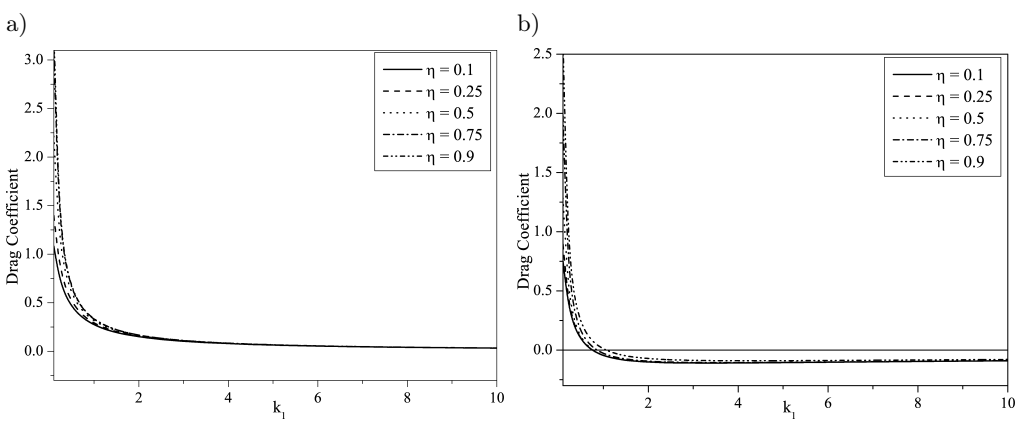

Fig. 5. Variation of the drag coefficient D_N with normalized permeability k_1 for various values of $\eta = a/b$: a) $\beta = 0.0$, $\gamma = 0.0$, $\sigma = 0.0$; b) $\beta = 0.15$, $\gamma = 0.1$, $\sigma = 0.5$.

coefficient σ. It is observed that there is a slight increase in the drag coefficient as η is increasing. Figure 5b presents the variation of the drag coefficient with effect of stress jump coefficient σ, it is noticed that the drag coefficient becomes negative after the critical permeability.

The wall correction factor W_c is defined as the ratio of the actual drag experienced by the particle in the enclosure and the drag on a particle in an infinite expanse of fluid. With the aid of Eqs. (5.2) and (5.3) this becomes

$$W_c = \frac{D}{D_\infty}. \tag{5.4}$$

Note that $W_c = 1$ as $\eta = 0$ and $W_c \geq 1$ as $0 < \eta \leq 1$.

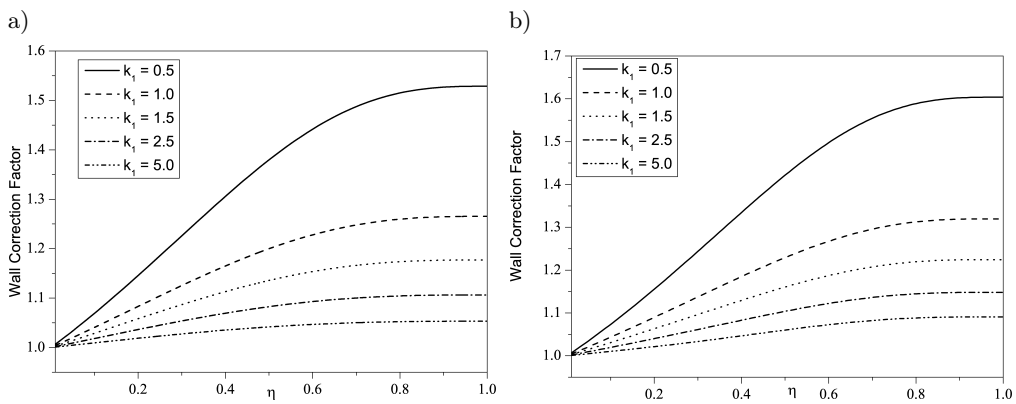

FIG. 6. Variation of the wall correction factor with $\eta = a/b$ for various values of normalized permeability k_1: a) $\beta = 0.0$, $\gamma = 0.0$, $\sigma = 0$; b) $\beta = 0.15$, $\gamma = 0.1$,$\sigma = 0$.

The variation of wall correction factor W_c against the separation parameter η with continuity of tangential stress ($\sigma = 0$) for various values of normalized permeability k_1 is shown in Fig. 6. Figure 6a, shows the variation of W_c with η for the motion of porous sphere in a spherical container for various values of k_1. The separation parameter η ($= a/b$) reflecting the extent of closeness between the particle and the cavity wall, ranges from 0 (far apart) to 1 (in contact). It is observed in the figure that, as η increases, the wall correction factor increases. For $k_1 > 2$, the particle mobility varies slowly with the separation parameter η, compared with the case of lower permeability (or greater α). Similar behavior is observed in Fig. 6b when the porous sphere and spherical container are perturbed. The effect of the stress jump coefficient σ and separation parameter η on wall correction factor W_c has been plotted in Fig. 7. It is observed that the wall corrector factor increases as η increases for negative values of stress jump coefficient σ and for positive values of σ, $W_c < 1$ for high permeability which is not physically possible.

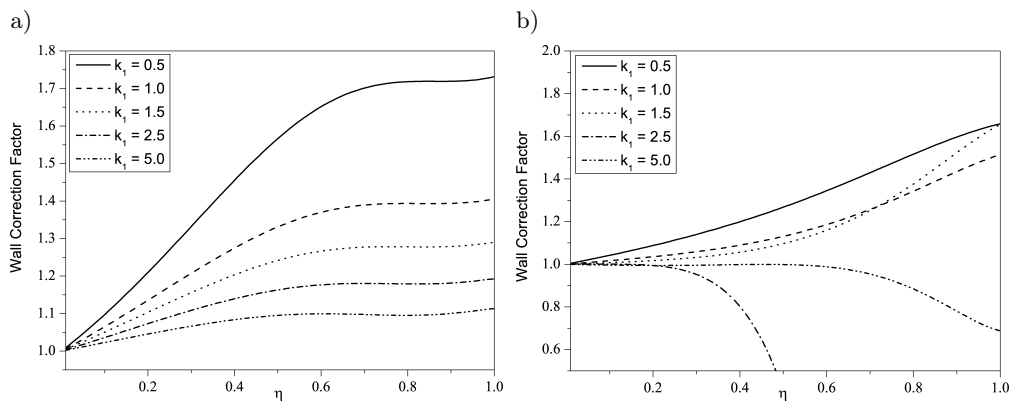

Fig. 7. Variation of the wall correction factor with $\eta = a/b$ for various values of normalized permeability k_1: a) $\beta = 0.15$, $\gamma = 0.1$, $\sigma = -0.3$; b) $\beta = 0.15$, $\gamma = 0.1$, $\sigma = 0.3$.

6. Special cases

Case (i). *A porous sphere in a spherical container.* If $\beta_m = 0$ and $\gamma_m = 0$ for $m > 2$, the inner and outer approximate spheres reduce to spheres and the drag on porous sphere in spherical contianer is

$$D = 4\pi\mu U a D_2. \tag{6.1}$$

If $\sigma = 0$, i.e., the continuity of the shear stress, the drag on the porous sphere (6.1) reduces to

$$D = 24\pi\mu U a\alpha^2\big[\alpha\left(15\eta^5 + \alpha^2(\eta^5 - 1)\right)\cosh\alpha - \left(15\eta^5 + \alpha^2(6\eta^5 - 1)\right)\sinh\alpha\big]/L_1, \tag{6.2}$$

where

$$\begin{aligned} L_1 = \alpha\big(&-270\eta^5 + \alpha^4(\eta-1)^4(4\eta^2 + 7\eta + 4) \\ &+ 6\alpha^2(10\eta^6 - 21\eta^5 + 10\eta^3 + 1)\big)\cosh\alpha \\ &- \big(-270\eta^5 + 3\alpha^4(\eta-1)^3\eta(8\eta^2 + 9\eta + 3) \\ &+ 6\alpha^2(10\eta^6 - 36\eta^5 + 10\eta^3 + 1)\big)\sinh\alpha, \end{aligned}$$

which agrees with the drag on the porous sphere in spherical container case obtained in [27] and [29].

If $b \to \infty$ (or $\eta \to 0$), we obtain drag on a porous sphere in the case of streaming in an unbounded medium. Applying the limit as $\eta \to 0$ to (6.2), we get

$$D_\infty = \frac{12\pi\mu U a\alpha^2\left(-\alpha\cosh\alpha + \sinh\alpha\right)}{\alpha(3 + 2\alpha^2)\cosh\alpha - 3\sinh\alpha}, \tag{6.3}$$

which agrees with the drag on the porous sphere case derived by BRINKMAN [19], NEALE *et al.* [41] and QIN and KALONI [42].

CASE (ii). *A porous oblate spheroid in an oblate spheroidal container.* Consider the motion of a porous oblate spheroid particle at the instant it passes the centre of an oblate spheroidal container. We take the equation of surface of the porous oblate spheroid to be

$$\frac{x^2+y^2}{c^2}+\frac{z^2}{c^2(1-\varepsilon)^2}=1 \tag{6.4}$$

whose equatorial radius is c in which ε is so small that ε^2 and higher powers may be neglected. Following HAPPEL and BRENNER [2] its polar equation can be written in the form $r=a[1+2\varepsilon\vartheta_2(\zeta)]$, where $a=c(1-\varepsilon)$ (see [2, p. 144]). Similarly, the equation of an oblate spheroidal container can be noted in the form $r=b[1+2\varepsilon\vartheta_2(\zeta)]$.

Using (4.1) and (4.2), the expressions for stream functions can be determined. The drag on the oblate spheroidal particle is

$$D=4\pi\mu Ua[D_2+(D_2+(2/5L)(\Delta_2+\Delta_3))\varepsilon]. \tag{6.5}$$

The volume of the spheroid defined by Eq. (6.5) is $(4/3)\pi c^3(1-\varepsilon)$, and a sphere of equal volume can be obtained by choosing the radius equal to $c(1-\varepsilon/3)$ (with ε^2 and higher powers neglected) (see [2, p. 144]). The non-dimensional drag on such a sphere is $4\pi\mu U(1-\varepsilon/3)D_2$ and this is clearly less than the drag on the spheroid. Similar comment holds for the drag on the sphere of equal surface area as that of the spheroid. These two conclusions are the same as in the case of viscous fluid [2] and micropolar fluid [43]. Further, the volume of the spheroid in terms of a is $(4\pi/3)a^3/(1-\varepsilon)^2$ which is larger than the volume of the sphere $4\pi a^3/3$. Since the spheroid is larger than the sphere, it interacts more with the container, and the drag increases.

The variation of the drag coefficient $D_N=D/(4\pi\mu Ua)$ for various values of normalized permeability k_1 and ε is shown in Fig. 8a for fixed value of $\sigma=0$. It can be observed that the drag coefficient is decreasing as the permeability is increasing. There is a slight increase in the drag coefficient as the deformation parameter ε is increasing. It is interesting to note that the drag coefficient on the porous sphere ($\varepsilon=0$) is less than that of the drag on the porous oblate spheroid. In Fig. 8b, the drag coefficient increases as η increases for particular value of stress jump coefficient. The variation of the drag coefficient D_N for various values of k_1 and σ is shown in Fig. 9, for fixed values of ε. It is observed that the drag coefficient decreases as the permeability increases for negative values of stress jump coefficient σ and for positive values of σ, the drag is positive only for a particular range of permeability.

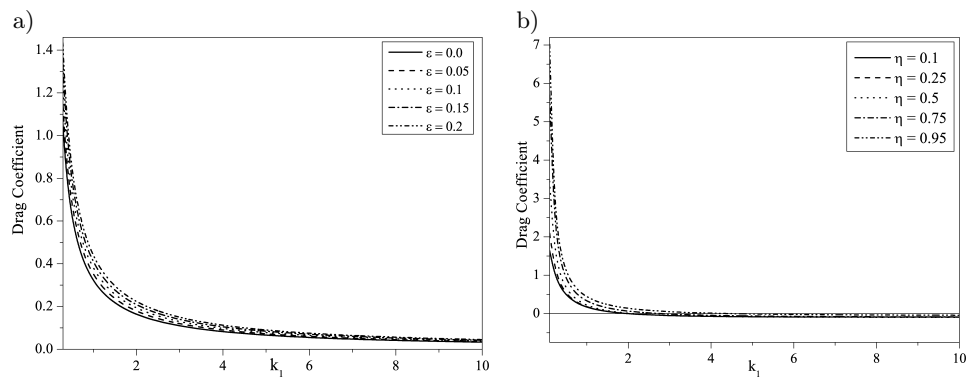

Fig. 8. Variation of the drag coefficient D_N with normalized permeability k_1 (*oblate spheroid*): a) for various values of ε, $\sigma = 0$, $\eta = 0.6$; b) for various values of η, $\sigma = 0.3$, $\varepsilon = 0.75$.

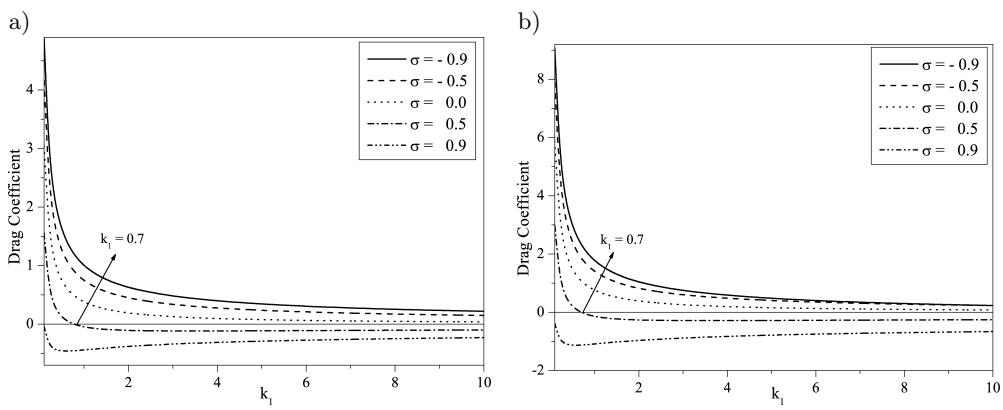

Fig. 9. Variation of the drag coefficient D_N with normalized permeability k_1 (*oblate spheroid*) for various values of σ: a) $\varepsilon = 0.1$, $\eta = 0.6$; b) $\varepsilon = 0.75$, $\eta = 0.6$.

7. Conclusions

An exact solution for the problem of the motion of a porous approximate sphere in an approximate spherical container is obtained by considering the Brinkman's model in the porous region and Stokes equations in the liquid region. At the porous-liquid interface Ochoa-Tapia's stress jump boundary condition, continuity of the normal velocity and continuity of the pressure have been used. An expression for the drag on the porous particle in a container and wall correction factor are obtained. It is observed that the drag coefficient on the porous sphere is less than that on the drag of the porous approximate sphere in presence of spherical cavity. The drag is decreasing as the permeability is

increasing. The drag is decreasing as the stress jump coefficient σ is increasing. For negative values of σ, the drag is always positive for any permeability. But for positive values of σ, the drag is positive only for a particular range of permeability. Hence, we conclude that stress jump condition, characterized by a stress jump coefficient, has a significant impact on the drag force.

8. Appendix

Applying the boundary conditions (3.6) and (3.7) to the first order in β_m and γ_m, we obtain the following system of algebraic equations:

$$\begin{aligned}(8.1)\qquad &\left[A_2+B_2+C_2+D_2-E_2-I_{3/2}(\alpha)F_2\right]\vartheta_2(\zeta)\\ &+\left[2A_2-B_2+4C_2+D_2-2E_2\right]\beta_m\vartheta_m(\zeta)\vartheta_2(\zeta)\\ &+\sum_{n=3}^{\infty}\left[A_n+B_n+C_n+D_n-E_n-I_{n-1/2}(\alpha)F_n\right]\vartheta_n(\zeta)=0,\end{aligned}$$

$$\begin{aligned}(8.2)\qquad &\left[2A_2-B_2+4C_2+D_2-2E_2+\left[I_{3/2}(\alpha)-\alpha I_{1/2}(\alpha)\right]F_2\right]\vartheta_2(\zeta)\\ &+\left[2A_2+2B_2+12C_2-2E_2-I_{3/2}(\alpha)F_2\right]\beta_m\vartheta_m(\zeta)\vartheta_2(\zeta)\\ &+\sum_{n=3}^{\infty}[nA_n-(n-1)B_n+(n+2)C_n-(n-3)D_n-nE_n\\ &+\left[(n-1)I_{n-1/2}(\alpha)-\alpha I_{n-3/2}(\alpha)\right]F_n\Big]\vartheta_n(\zeta)=0,\end{aligned}$$

$$\begin{aligned}(8.3)\qquad &[-2A_2-2B_2-12C_2+2(1-\alpha\sigma)E_2\\ &+[(\alpha^2+\alpha\sigma+2)I_{3/2}(\alpha)-\alpha^2\sigma I_{1/2}(\alpha)]F_2]\vartheta_2(\zeta)\\ &+[6B_2-24C_2-2\alpha\sigma E_2-(4+\alpha\sigma)I_{3/2}(\alpha)F_2]\beta_m\vartheta_m(\zeta)\vartheta_2(\zeta)\\ &+\sum_{n=3}^{\infty}[-n(n-1)A_n-n(n-1)B_n\\ &-(n+1)(n+2)C_n-(n-2)(n-3)D_n+n((n-1)-\alpha\sigma)E_n\\ &+[((n+\alpha\sigma)(n-1)+\alpha^2)I_{n-1/2}(\alpha)-\alpha^2\sigma I_{n-3/2}(\alpha)]F_n]\vartheta_n(\zeta)=0,\end{aligned}$$

$$\begin{aligned}(8.4)\qquad &-\left[10C_2+D_2+\alpha^2E_2\right]P_1(\zeta)-\left[10C_2-2D_2+\alpha^2E_2\right]P_1(\zeta)\beta_m\vartheta_m(\zeta)\\ &-\sum_{n=3}^{\infty}\left[\left(\frac{4n+2}{n-1}\right)C_n-\left(\frac{6-4n}{n}\right)D_n+\frac{\alpha^2}{(n-1)}E_n\right]P_{n-1}(\zeta)=0,\end{aligned}$$

$$
\begin{aligned}
(8.5)\qquad & \left[\eta^{-2}A_2+\eta B_2+\eta^{-4}C_2+\eta^{-1}D_2-\eta^{-2}\right]\vartheta_2(\zeta)\\
&+\left[2\eta^{-2}A_2-\eta B_2+4\eta^{-4}C_2+\eta^{-1}D_2-2\eta^{-2}\right]\gamma_m\vartheta_m(\zeta)\vartheta_2(\zeta)\\
&+\sum_{n=3}^{\infty}\left[\eta^{-n}A_n+\eta^{n-1}B_n+\eta^{-n-2}C_n+\eta^{n-3}D_n\right]\vartheta_n(\zeta)=0,
\end{aligned}
$$

$$
\begin{aligned}
(8.6)\qquad & \left[2\eta^{-1}A_2-\eta^2B_2+4\eta^{-3}C_2+D_2-2\eta^{-1}\right]\vartheta_2(\zeta)\\
&+\left[2\eta^{-1}A_2+2\eta^2B_2+12\eta^{-3}C_2-2\eta^{-1}\right]\gamma_m\vartheta_m(\zeta)\vartheta_2(\zeta)\\
&+\sum_{n=3}^{\infty}[n\eta^{-n+1}A_n-(n-1)\eta^nB_n\\
&+(n+2)\eta^{-n-1}C_n-(n-3)\eta^{n-2}D_n]\vartheta_n(\zeta)=0.
\end{aligned}
$$

Equating the leading coefficients in (8.1)–(8.6) to zero and solving the resulting system of equations, we obtain

$$
\begin{aligned}
A_2=\ & \big[-\alpha\left(270\eta^5+6\alpha^2(21\eta^5-5\eta^3-1)+\alpha^3(\alpha+\sigma)(9\eta^5-5\eta^3-4)\right.\\
&\left.-6\alpha\sigma(9\eta^5+5\eta^3+1)\right)\cosh\alpha+\left(270\eta^5+15\alpha^4\eta^3(3\eta^2-1)\right.\\
&+6\alpha^2(36\eta^5-5\eta^3-1)+\alpha\sigma\left(\alpha^4(9\eta^5-5\eta^3-4)\right.\\
&\left.\left.-3\alpha^2(3\eta^5+5\eta^3+2)-6(9\eta^5+5\eta^3+1)\right)\right)\sinh\alpha\big]/L,
\end{aligned}
$$

$$
\begin{aligned}
B_2=\ & -2\alpha\left[\alpha\left(\alpha^2(\alpha+\sigma)(\eta^3-1)+3\alpha(5\eta^3-2)-6\sigma(5\eta^3+1)\right)\cosh\alpha\right.\\
&-\left(3\alpha(5\eta^3-2)+3\alpha^3(2\eta^3-1)+\sigma\left(\alpha^4(\eta^3-1)-3\alpha^2(3\eta^2+1)\right.\right.\\
&\left.\left.-6(5\eta^3+1)\right)\right)\sinh\alpha\Big]/L,
\end{aligned}
$$

$$
\begin{aligned}
C_2=\ & 3\alpha\eta^3\left[\alpha(\alpha+\sigma)(6\eta^2+\alpha^2(\eta^2-1))\cosh\alpha-\left(6\eta^2(\alpha+\sigma)+\alpha^2(\alpha\right.\right.\\
&\left.\left.+\sigma)(3\eta^2-1)+\alpha^4\sigma(\eta^2-1)\right)\sinh\alpha\right]/L,
\end{aligned}
$$

$$
\begin{aligned}
D_2=\ & 6\alpha[\alpha(15\eta^5(\alpha-2\sigma)+\alpha^2(\alpha+\sigma)(\eta^5-1))\cosh\alpha\\
&-(15\eta^5(\alpha-2\sigma)+\alpha^3(6\eta^5-1)+\alpha^4\sigma(\eta^5-1)-\alpha^2\sigma(9\eta^5+1))\sinh\alpha]/L,
\end{aligned}
$$

$$
\begin{aligned}
E_2=\ & -6[\alpha(45\eta^5+\alpha(\alpha+\sigma)(6\eta^5-5\eta^3-1))\cosh\alpha\\
&-(45\eta^5+\alpha^2(21\eta^5-5\eta^3-1)+\alpha\sigma(1+\alpha^2)(6\eta^5-5\eta^3-1))\sinh\alpha]/L,
\end{aligned}
$$

$$
F_2=3\sqrt{2\pi}\alpha^{5/2}\left(\alpha(3\eta^5-5\eta^3+2)-2\sigma(6\eta^5-5\eta^3-1)\right)/L,
$$

where

$$
\begin{aligned}
L = {} & \alpha(-270\eta^5 + \alpha^3(\alpha+\sigma)(\eta-1)^4(4\eta^2+7\eta+4) \\
& + 6\alpha\sigma(-20\eta^6 + 9\eta^5 + 10\eta^3 + 1) + 6\alpha^2(10\eta^6 - 21\eta^5 + 10\eta^3 + 1))\cosh\alpha \\
& - (-270\eta^5 + \alpha^5\sigma(\eta-1)^4(4\eta^2+7\eta+4) + 3\alpha^4(\eta-1)^3\eta(8\eta^2+9\eta+3) \\
& + 6\alpha\sigma(-20\eta^6 + 9\eta^5 + 10\eta^3 + 1) + 3\alpha^3\sigma(-12\eta^6 + 3\eta^5 + 10\eta^3 - 3\eta + 2) \\
& + 6\alpha^2(10\eta^6 - 36\eta^5 + 10\eta^3 + 1))\sinh\alpha.
\end{aligned}
$$

To obtain the remaining arbitrary constants A_n, B_n, C_n, D_n, E_n, F_n, we require the following identities (see [2, p. 142]):

$$\vartheta_m(\zeta)\vartheta_2(\zeta) = b_{m-2}\vartheta_{m-2}(\zeta) + b_m\vartheta_m(\zeta) + b_{m+2}\vartheta_{m+2}(\zeta), \tag{8.7}$$

$$\vartheta_m(\zeta)P_1(\zeta) = a_{m-2}P_{m-3}(\zeta) + a_mP_{m-1}(\zeta) + a_{m+2}P_{m+1}(\zeta), \tag{8.8}$$

where

$$
\begin{aligned}
b_{m-2} &= -\frac{(m-2)(m-3)}{2(2m-1)(2m-3)}, & b_m &= \frac{m(m-1)}{(2m+1)(2m-3)}, \\
b_{m+2} &= -\frac{(m+1)(m+2)}{2(2m-1)(2m+1)}, & a_{m-2} &= \frac{(m-2)}{(2m-1)(2m-3)}, \\
a_m &= \frac{1}{(2m+1)(2m-3)}, & a_{m+2} &= -\frac{(m+1)}{(2m-1)(2m+1)}.
\end{aligned} \tag{8.9}
$$

Using these in (8.1)–(8.6), we obtain

$$A_n = B_n = C_n = D_n = E_n = F_n = 0 \qquad \text{for } n \neq m-2, m, m+2 \tag{8.10}$$

and when $n = m-2, m, m+2$, we have the following system of equations:

$$
\begin{aligned}
A_n + B_n + C_n + D_n - E_n - I_{n-1/2}(\alpha)F_n & \\
= -\left[2A_2 - B_2 + 4C_2 + D_2 - 2E_2\right]\beta_m b_n, &
\end{aligned} \tag{8.11}
$$

$$
\begin{aligned}
nA_n - (n-1)B_n + (n+2)C_n - (n-3)D_n - nE_n & \\
+ \left[(n-1)I_{n-1/2}(\alpha) - \alpha I_{n-3/2}(\alpha)\right]F_n & \\
= -\left[2A_2 + 2B_2 + 12C_2 - 2E_2 - I_{3/2}(\alpha)F_2\right]\beta_m b_n, &
\end{aligned} \tag{8.12}
$$

$$
\begin{aligned}
-n(n-1)A_n - n(n-1)B_n - (n+1)(n+2)C_n & \\
- (n-2)(n-3)D_n + n((n-1) - \alpha\sigma)E_n & \\
+ \left[((n+\alpha\sigma)(n-1) + \alpha^2)I_{n-1/2}(\alpha) - \alpha^2\sigma I_{n-3/2}(\alpha)\right]F_n & \\
= -\left[6B_2 - 24C_2 - 2\alpha\sigma E_2 - (4+\alpha\sigma)I_{3/2}(\alpha)F_2\right]\beta_m b_n, &
\end{aligned} \tag{8.13}
$$

$$-\left(\frac{4n+2}{n-1}\right)C_n+\left(\frac{6-4n}{n}\right)D_n-\frac{\alpha^2}{(n-1)}E_n = \left[10C_2-2D_2+\alpha^2E_2\right]\beta_m a_n, \tag{8.14}$$

$$\eta^{-n}A_n+\eta^{n-1}B_n+\eta^{-n-2}C_n+\eta^{n-3}D_n = -\left[2\eta^{-2}A_2-\eta B_2+4\eta^{-4}C_2+\eta^{-1}D_2-2\eta^{-2}\right]\gamma_m b_n, \tag{8.15}$$

$$n\eta^{-n+1}A_n-(n-1)\eta^nB_n+(n+2)\eta^{-n-1}C_n-(n-3)\eta^{n-2}D_n = -\left[2\eta^{-1}A_2+2\eta^2B_2+12\eta^{-3}C_2-2\eta^{-1}\right]\gamma_m b_n. \tag{8.16}$$

The above system of equations is solved using Mathematica and the values of A_n, B_n, C_n, D_n, E_n, and F_n, for $n=m-2,m,m+2$ are obtained. These constants contain the coefficients β_m and γ_m. As the expressions are cumbersome, they are not presented here.

The expression for the constant D_2' appearing in Eq. (5.2) is

$$D_2'=\frac{1}{5L}\left(\Delta_2\beta_2+\Delta_3\gamma_2\right)+\frac{2}{35L}\left(\Delta_4\beta_4+\Delta_5\gamma_4\right), \tag{8.17}$$

where

$$\begin{aligned}
\Delta_2 = \big(&-12\alpha(\alpha^2[10125\alpha\eta^{10}+270\alpha^3\eta^5(11\eta^5-10\eta^3-1)\\
&+9\alpha^5(26\eta^{10}-50\eta^8+25\eta^6-2\eta^5+1)+\alpha^7(\eta-1)^4(3\eta^3+6\eta^2+4\eta+2)^2\\
&+(90\eta^5+\alpha^2(3\eta^5-5\eta^3+2))(-135\eta^5-9\alpha^2(\eta^5-1)+2\alpha^4(3\eta^5-5\eta^3+2))\sigma\\
&+\alpha\sigma^2(810(4\eta^{10}+5\eta^8+\eta^5)+\alpha^4(\eta-1)^4(3\eta^3+6\eta^2+4\eta+2)^2\\
&+9\alpha^2(6\eta^{10}+5\eta^8-50\eta^6+43\eta^5-5\eta^3+1))]\cosh^2\alpha\\
&+\alpha[6\alpha(-3375\eta^{10}+3\alpha^4\eta^5(150\eta^3-25\eta-13)-5\alpha^6\eta^3(3\eta^7-8\eta^5+2\eta^2-2)\\
&+90\alpha^2\eta^5(10\eta^3+1))+(24300\eta^{10}+2\alpha^8(5\eta^3-2)(6\eta^5-5\eta^3+2)\\
&-18\alpha^4(42\eta^{10}-31\eta^5-5\eta^3+2)\\
&-3\alpha^6(123\eta^{10}-255\eta^8+100\eta^6+69\eta^5-45\eta^3+8))\sigma\\
&+2\alpha(-810\eta^8(4\eta^2+5)+\alpha^6(5\eta^3-2)(6\eta^5-5\eta^3+2)\\
&-9\alpha^2\eta^3(126\eta^7+155\eta^5-50\eta^3-5)\\
&-3\alpha^4(39\eta^{10}-40\eta^8-75\eta^6+82\eta^5-10\eta^3+4))\sigma^2]\cosh\alpha\sinh\alpha\\
&+[10125\alpha\eta^{10}+270\alpha^3\eta^5(36\eta^5-10\eta^3-1)\\
&+9\alpha^5(321\eta^{10}-250\eta^8+25\eta^6+28\eta^5+1)
\end{aligned} \tag{8.18}$$

$$
\begin{aligned}
&+\alpha^7(\eta-1)^2(87\eta^5-25\eta^3-2)(3\eta^3+6\eta^2+4\eta+2)\\
&+\sigma(-12150\eta^{10}-135\alpha^2\eta^5(69\eta^5-5\eta^3-4)\\
&-9\alpha^4(123\eta^{10}+45\eta^8-21\eta^5+5\eta^3-2)+30\alpha^8\eta^3(3\eta^7-8\eta^5+5\eta^3+2\eta^2-2)\\
&+\alpha^6(396\eta^{10}-630\eta^8+250\eta^6+63\eta^5-95\eta^3+16))\\
&+\alpha\sigma^2(810\eta^5(4\eta^5+5\eta^3+1)+\alpha^8(\eta-1)^4(3\eta^3+6\eta^2+4\eta+2)^2\\
&+\alpha^6(36\eta^{10}-45\eta^8-100\eta^6+153\eta^5-55\eta^3+11)\\
&+5\alpha^4(117\eta^{10}+48\eta^8-95\eta^6+114\eta^5-8\eta^3+4)\\
&+9\alpha^2(246\eta^{10}+305\eta^8-50\eta^6+103\eta^5-5\eta^3+1))]\sinh^2\alpha\\
&-3\alpha^2[3\alpha^4+25\alpha^6\eta^6+9\alpha^2(235+37\alpha^2)\eta^{10}\\
&+3\alpha\eta^5((\alpha^6-585)\eta^5+(75-70\alpha^2)\eta^3+60)\sigma\\
&+3(\alpha^2+(90+73\alpha^2)\eta^5+\alpha^6\eta^{10})\sigma^2]\sinh 2\alpha\big)/L,
\end{aligned}
$$

$$
\begin{aligned}
\Delta_3 = \big(&12\alpha^2\eta(\alpha(30\alpha\eta^2(\eta^3-1)+\alpha^2(\alpha+\sigma)(2\eta^5-5\eta^2+3)\\
&-30\eta^2\sigma(2\eta^3+1))\cosh\alpha-(30\alpha\eta^2(\eta^3-1)+3\alpha^3(4\eta^5-5\eta^2+1)\\
&-30\eta^2\sigma(2\eta^3+1)+\alpha^4\sigma(2\eta^5-5\eta^2+3)\\
&-3\alpha^2\sigma(6\eta^5+5\eta^2-1))\sinh\alpha)^2\big)/L,
\end{aligned}
\tag{8.19}
$$

$$
\begin{aligned}
\Delta_4 = \big(&3\alpha(\alpha^2[\alpha^3(\eta-1)^2(540\eta^5+\alpha^4(3\eta^5-5\eta^3+2)\\
&+9\alpha^2(7\eta^5-5\eta^3-2))(3\eta^3+6\eta^2+4\eta+2)\\
&+2\sigma(4050\eta^{10}-135\alpha^2\eta^5(17\eta^5-15\eta^3-2)\\
&+9\alpha^4(11\eta^{10}-35\eta^8+43\eta^5-15\eta^3-4)+\alpha^6(\eta-1)^4(3\eta^3+6\eta^2+4\eta+2)^2)\\
&+\alpha\sigma^2(540\eta^5(21\eta^5-5\eta^3-1)+\alpha^4(\eta-1)^4(3\eta^3+6\eta^2+4\eta+2)^2\\
&-18\alpha^2(12\eta^{10}-15\eta^8+25\eta^6-39\eta^5+15\eta^3+2))]\cosh^2\alpha\\
&+[\alpha^3(\eta-1)^2(540\eta^5+9\alpha^2(47\eta^5-5\eta^3-2)\\
&+\alpha^4(87\eta^5-25\eta^3-2))(3\eta^3+6\eta^2+4\eta+2)\\
&+2\sigma(4050\eta^{10}-9\alpha^4(129\eta^{10}-115\eta^8-83\eta^5+15\eta^3+4)\\
&+135\alpha^2\eta^5(3\eta^5+15\eta^3+2)+15\alpha^8\eta^3(3\eta^7-8\eta^5+5\eta^3+2\eta^2-2)\\
&-\alpha^6(207\eta^{10}+90\eta^8-125\eta^6-279\eta^5+85\eta^3+22))\\
&+\alpha\sigma^2(540\eta^5(21\eta^5-5\eta^3-1)+\alpha^8(\eta-1)^4(3\eta^3+6\eta^2+4\eta+2)^2
\end{aligned}
\tag{8.20}
$$

$$
\begin{aligned}
&- 2\alpha^6(27\eta^{10} - 15\eta^8 + 50\eta^6 - 129\eta^5 \\
&+ 65\eta^3 + 2) + 5\alpha^4(225\eta^{10} - 42\eta^8 - 95\eta^6 + 168\eta^5 - 68\eta^3 - 8) \\
&+ 18\alpha^2(408\eta^{10} - 85\eta^8 - 25\eta^6 + 19\eta^5 - 15\eta^3 - 2))]\sinh^2\alpha \\
&- \alpha[3\alpha^3(\eta-1)^2((5\alpha^4 + 81\alpha^2 + 180)\eta^5 - 5\alpha^2(3+\alpha^2)\eta^3 - 6\alpha^2) \\
&\times (3\eta^3 + 6\eta^2 + 4\eta + 2) + \sigma(8100\eta^{10} - 270\alpha^2\eta^5(7\eta^5 - 15\eta^3 - 2) \\
&- 18\alpha^4(84\eta^{10} - 40\eta^8 - 63\eta^5 + 15\eta^3 + 4) \\
&+ \alpha^8(\eta-1)^4(3\eta^3 + 6\eta^2 + 4\eta + 2)^2 \\
&+ 3\alpha^6(39\eta^{10} - 115\eta^8 + 50\eta^6 + 67\eta^5 - 35\eta^3 - 6)) \\
&+ \alpha\sigma^2(540\eta^5(21\eta^5 - 5\eta^3 - 1) + \alpha^6(\eta-1)^4(3\eta^3 + 6\eta^2 + 4\eta + 2)^2 \\
&- 3\alpha^4(21\eta^{10} - 10\eta^8 + 75\eta^6 - 152\eta^5 + 60\eta^3 + 6) \\
&+ 18\alpha^2(198\eta^{10} - 35\eta^8 - 25\eta^6 + 29\eta^5 - 15\eta^3 - 2))]\sinh 2\alpha\big)/L,
\end{aligned}
$$

$$
\begin{aligned}
\Delta_5 = \big(&-3\alpha^2\eta(\alpha(30\alpha\eta^2(\eta^3-1) + \alpha^2(\alpha+\sigma)(2\eta^5 - 5\eta^2 + 3) \\
&- 30\eta^2\sigma(2\eta^3+1))\cosh\alpha - (30\alpha\eta^2(\eta^3-1) + 3\alpha^3(4\eta^5 - 5\eta^2 + 1) \\
&- 30\eta^2\sigma(2\eta^3+1) + \alpha^4\sigma(2\eta^5 - 5\eta^2 + 3) \\
&- 3\alpha^2\sigma(6\eta^5 + 5\eta^2 - 1))\sinh\alpha)^2\big)/L.
\end{aligned} \tag{8.21}
$$

The expressions for the constants Δ_6, Δ_7, Δ_8 and Δ_9 appearing in Eq. (5.3) are defined as

$$
\Delta_6 = \alpha(3+2\alpha^2)(\alpha+\sigma)\cosh\alpha - (3\alpha + (3 + 3\alpha^2 + 2\alpha^4)\sigma)\sinh\alpha, \tag{8.22}
$$

$$
\Delta_7 = 3\alpha^2(-\alpha(\alpha+\sigma)\cosh\alpha + (\alpha + \sigma + \alpha^2\sigma)\sinh\alpha), \tag{8.23}
$$

$$
\begin{aligned}
\Delta_8 = 3\alpha^2(&9\alpha^2 - 13\alpha^4 - 4\alpha^6 - 2\alpha\sigma(4\alpha^4 + \alpha^2 - 9) \\
&+ (4\alpha^6 + 7\alpha^4 + 11\alpha^2 + 9)\sigma^2 - (\alpha^2(4\alpha^4 + 5\alpha^2 + 9) \\
&+ 2\alpha\sigma(4\alpha^4 + 17\alpha^2 + 9) + (4\alpha^6 + 15\alpha^4 + 29\alpha^2 + 9)\sigma^2)\cosh 2\alpha \\
&+ 2\alpha(\alpha+\sigma)(9\alpha + (3+2\alpha^2)^2\sigma)\sinh 2\alpha)/(2\Delta_6),
\end{aligned} \tag{8.24}
$$

$$
\begin{aligned}
\Delta_9 = 3\alpha^2\big(&(\alpha^6 - 8\alpha^4 + 9\alpha^2) + (2\alpha^5 - 7\alpha^3 + 18\alpha)\sigma \\
&- (\alpha^6 - 2\alpha^4 - \alpha^2 - 9)\sigma^2 + (\alpha^2(\alpha^4 - 10\alpha^2 - 9) \\
&+ \alpha\sigma(2\alpha^4 - 29\alpha^2 - 18) + (\alpha^6 - 19\alpha^2 - 9)\sigma^2)\cosh 2\alpha \\
&- \alpha(\alpha+\sigma)(-18\alpha + (\alpha^2 - 6)(3 + 2\alpha^2)\sigma)\sinh 2\alpha)/(2\Delta_6).
\end{aligned} \tag{8.25}
$$

References

1. C.W. Oseen, *Hydrodynamik*, Akademische Verlagsgesellschaft, Leipzig, 1927.
2. J. Happel, H. Brenner, *Low Reynolds Number Hydrodynamics*, Prentice-Hall, Englewood Cliffs, N.J. 1965.
3. S. Kim, S.J. Karrila, *Microhydrodynamics: Principles and Selected Applications*, Butterworth-Heinemann, Boston, MA, USA 1991.
4. R.B. Jones, *Dynamics of a colloid in a spherical cavity*, [in:] Theoretical Methods for Micro Scale Viscous Flows, eds. Francois Feuillebois and Antoine Sellier, Transworld Research Network, 2009.
5. E. Cunningham, *On the velocity of steady fall of spherical particles through fluid medium*, Proc. Roy. Soc. London Ser., **83**, 357–369, 1910.
6. W.E. Williams, *On the motion of a sphere in a viscous fluid*, Philos. Mag., **29**, 526–550, 1915.
7. W.L. Haberman, R.M. Sayre, *Wall effects for rigid and fluid spheres in slow motion with a moving liquid. David Taylor model*, Basin Report No 1143, Washington, DC, 1958.
8. H. Ramkissoon, K. Rahaman, *Non-Newtonian fluid sphere in a spherical container*, Acta Mech., **149**, 239–245, 2001.
9. H. Ramkissoon, K. Rahaman, *Wall effects on a spherical particle*, Int. J. Eng. Sci., **41**, 283–290, 2003.
10. C. Maul, S. Kim, *Image systems for a Stokeslet inside a rigid spherical container*, Phys. Fluids, **6**, 2221–2223, 1994.
11. C. Maul, S. Kim, *Image of a point force in a spherical container and its connection to the Lorentz reflection formula*, J. Eng. Math., **30**, 119–130, 1996.
12. J.R. Blake, *A spherical envelope approach to ciliary propulsion*, J. Fluid Mech., **46**, 199–208, 1971.
13. B.U. Felderhof, A. Sellier, *Mobility matrix of a spherical particle translating and rotating in a viscous fluid confined in a spherical cell, and the rate of escape from the cell*, J. Chem. Phys., **136**, 054703, 2012.
14. D.D. Joseph, L.N. Tao, *The effect of permeability in the slow motion of a porous sphere in a viscous liquid*, Z. Angew. Math. Mech., **44**, 361–364, 1964.
15. G.S. Beavers, D.D. Joseph, *Boundary conditions at a naturally permeable wall*, J. Fluid Mech., **30**, 197–207, 1967.
16. P.G. Saffman, *On the boundary condition at the surface of a porous medium*, Stud. Appl. Math., **50**, 93–101, 1971.
17. B.S. Padmavathi, T. Amarnath, D. Palaniappan, *Stokes flow about a porous spherical particle*, Arch. Mech., **46**, 191–199, 1994.
18. D.N. Sutherland, C.T. Tan, *Sedimentation of a porous sphere*, Chem. Engg. Sc., **25**, 1948–1950, 1970.
19. H.C. Brinkman, *A calculation of viscous force exerted by a flowing fluid on dense swarm of particles*, Appl. Sci. Res., **A1**, 27–34, 1957.

20. P. Debye, A.M. Bueche, *Intrinsic viscosity, diffusion and sedimentation rate of polymers in solution*, J. Chem. Phys., **16**, 6, 573–579, 1948.

21. G. Ooms, P.E. Mijulieff, H.L. Becker, *Frictional force exerted by a flowing fluid in a permeable particle with particular reference to polymer coils*, J. Chem. Phys., **53**, 4123–4130, 1970.

22. K. Matsumoto, A. Suganuma, *Settling velocity of a permeable model floc*, Chem. Eng. Sci., **32**, 445–447, 1977.

23. C.K.W. Tam, *The drag on a cloud of spherical particles in a low Reynolds number flow*, J. Fluid Mech., **38**, 537–546, 1969.

24. T.S. Lundgren, *Slow flow through stationary random beds and suspensions of spheres*, J. Fluid Mech., **51**, 273–299, 1972.

25. Y. Qin, P.N. Kaloni, *A Cartesian tensor solution of the Brinkman equation*, J. Eng. Math., **22**, 177–188, 1988.

26. T. Zlatanovski, *Axisymmetric creeping flow past a porous prolate spheroidal particle using the Brinkman model*, Q. J. Mech. Appl. Math., **52**, 1, 111–126, 1999.

27. H.J. Keh, J. Chou, *Creeping motion of a composite sphere in a concentric spherical cavity*, Chem. Eng. Sci., **59**, 407–415, 2004.

28. H.J. Keh, Y.S. Lu, *Creeping motions of a porous spherical shell in a concentric spherical cavity*, J. Fluids and Structures, **20**, 735–747, 2005.

29. D. Srinivasacharya, *Motion of a porous sphere in a spherical container*, C. R. Mecanique, **333**, 612–616, 2005.

30. S. Deo, B.R. Gupta, *Stokes flow past a swarm of porous approximately spheroidal particles with Kuwabara boundary condition*, Acta Mech., **203**, 241–254, 2009.

31. E.I. Saad, *Translation and rotation of a porous spheroid in a spheroidal container*, Can. J. Phys., **88**, 689–700, 2010.

32. D.A. Nield, *The limitations of the Brinkman-Forchheimer equation in modelling flow in a saturated porous medium and at an interface*, Int. J. Heat Fluid Flow, **12**, 269–272, 1991.

33. D. Tomer, S. Uri, *An apparent interface location as a tool to solve the porous interface flow problem*, Transp. Porous Med., **78**, 509–524, 2009.

34. J.A. Ochoa-Tapia, S. Whitaker, *Momentum transfer at the boundary between a porous medium and a homogeneous fluid – I, theoretical development*, Int. J. Heat and Mass-Transfer., **38**, 2635–2646, 1995.

35. J.A. Ochoa-Tapia, S. Whitaker, *Momentum transfer at the boundary between a porous medium and a homogeneous fluid – II, comparison with experiment*, Int. J. Heat Mass Transfer, **38**, 2647–2655, 1995.

36. A.V. Kuznetsov, *Analytical investigation of the fluid flow in the interface region between a porous media and a clear fluid in channels partially filled with porous medium*, Appl. Sci. Res., **56**, 53–67, 1996.

37. A.V. Kuznetsov, *Analytical investigation of Couette flow in a composite channel partially filled with a porous media and partially with a clear fluid*, Int. J. Heat Mass Transfer, **41**, 2556–2560, 1998.

38. F.J. Valdès-Parada, J.A. Ramírez, B. Goyeau, J.A. Ochoa-Tapia, *Computation of jump coefficients for momentum transfer between a porous medium and a fluid using a closed generalized transfer equation*, Transp. Porous Med., **78**, 439–457, 2009.

39. G.P. Raja Sekhar, A. Bhattacharyya, *Stokes flow inside a porous spherical shell: Stress jump boundary condition*, Z. Angew. Math. Phys., **56**, 475–496, 2005.

40. D. Srinivasacharya, *Flow past a porous approximate spherical shell.* Z. Angew. Math. Phys., **58**, 646–658, 2007.

41. G. Neale, N. Epstein, W. Nader, *Creeping flow relative to permeable spheres*, Chem. Engng. Sci., **28**, 1865–1874, 1973.

42. Q. Yu, P.N. Kaloni, *A Cartesian tensor solution of the Brinkman equation*, J. Eng. Math., **22**, 177–188, 1988.

43. T.K.V. Iyengar, D. Srinivasacharya, *Stokes flow of an incompressible micro-polar fluid past an approximate sphere*, Int. J. Engng. Sci., **31**, 153–161, 1993.

Received February 18, 2012; final revised version August 4, 2013.